PRESSURE FIELD GENERATED BY NON-SPHERICAL BUBBLE COLLAPSE

C. L. Chahine, Senior Research Scientist
Hydronautics, Incorporated
Laurel, Maryland

A. G. Bovis
Ingenieur de l'armement
STCAN, Bassin des Carenes
Paris, France

ABSTRACT

The method of matched asymptotic expansions is used to investigate the behavior of a collapsing bubble near a solid wall. Cases are studied in which the ratio ε between the initial spherical bubble radius and its distance from the wall is small. Expansions in powers of ε lead to a simple system of differential equations which is solved numerically. The bubble shape, the velocity potential and the pressure field are determined as functions of time. The deformation of the bubble is a singluar perturbation of the pressure field around it. A decrease in the value of ε augments the pressure on the solid wall by orders of magnitude. The influence of surface tension and the proximity of the wall, gas content and its law of compression, are investigated. The results are compared to previous investigations. One advantage of the method employed is the fact that it leads to a numerical solution which costs very little computer time. In addition, it can be extended very easily to more complex cases such as multi-bubble configurations or to walls coated with elastomeric coatings.

NOMENCLATURE

$a_0, a_1, \ldots a_n$	spherical contributions to the bubble wall equation
$b(t)$	distance between the fixed and the moving coordinate system
f_2, f_3	amplitude of non-spherical perturbations of type $\cos\theta$ of $R(\theta,t)$
g_3	amplitude of non spherical perturbation of type $P_2(\cos\theta)$ of R
h_2, h_3	amplitude of non spherical perturbation of type $\cos\theta$ of ϕ
K_3	amplitude of non spherical perturbations of type $P_2(\cos\theta)$ of R
K	polytropic coefficient
ℓ_o	initial bubble center to wall distance
$p(r,\theta,t)$	pressure field
$P_\infty(t)$	imposed ambient pressure
P_o	initial ambient pressure
P_v	vapor pressure
$P_g(t)$	noncondensable gas pressure
ΔP	characteristic value of the imposed pressure $\Delta P = P_{max} - P_o$

$q_0, q_1, \ldots q_n$		strengths of first and successive spherical sources
r		spherical coordinate
r'		$(r^2 + 4\ell^2 - 4r\ell\cos\theta)^{\frac{1}{2}}$
R_o		initial bubble radius
t		time
T		characteristic time scale $T = R_o \sqrt{\rho/\Delta P}$
P	=	$(P_o - P_v)/\Delta P$
$P_n(\cos\theta)$		Legendre polynomial of order n
$R(\theta,t)$		bubble wall equation
ρ		liquid density
γ		surface tension
ε	=	$R_o/\ell_o \ll 1$
$\phi(r,\theta,t)$		velocity potential in the moving system
$\phi_0, \phi_1, \ldots \phi_n$		successive expansions of ϕ
$\Phi_.$		characteristic velocity potential
W_e	=	$R_o \cdot \Delta P/2\gamma$

Superscripts

$\cdot$	time differentiation
$-$	non dimensional outer variable
$\sim$	non dimensional inner variable

INTRODUCTION

The modeling of cavitation erosion and noise, as well as the related scaling effects requires the knowledge of individual and collective bubble behavior. Most presently used modeling approaches are of a statistical nature and are based on a spherical bubble collapse theory developed by Rayleigh. This spherical model was extended by Plesset (1) to the case of a gas and vapor filled spherical bubble moving along with the surrounding fluid. However, in practical situations where cavitation is harmful, collective bubble collapse and the presence of nearby solid boundaries are fundamental. Observations of non-spherical bubble collapse have been made experimentally using high-speed photography (2-4). A high-speed re-entering jet is seen to be formed at the final stage of collapse. Pressure waves of higher maximum amplitude than those obtained in the spherical case are expected to be generated and to contribute to the jet damaging effect.

Despite its great practical importance, non-spherical bubble dynamics studies are not very advanced due to the complexity of the free boundary problem involved. Analytical solutions are unlikely at present. However, several important contributions do exist (5-8) which are either purely numerical or numerical with some analytical simplifications. These investigations succeeded in describing the re-entering jet formation, as well as its early evolution. The final stage of collapse could not be obtained due, either to numerical instabilities or to failure of the analytical mode. These calculations are very time consuming; thus they have not been extended to investigate the influence of different parameters, or to study complex configurations. In previous publications (4,9), we proposed then used matched asymptotic expansions to study the problem when the bubble radius is small compared to its distance from nearby boundaries. The behavior in the more complicated case where the two lengths are of the same order of magnitude, can be at least qualitatively deduced from the behavior of the solution when the small parameter approaches unity. This method is used here for the analysis of the collapse of an isolated bubble near a solid wall. A moving coordinate system attached to the bubble allows following the bubble deformation during the collapse for a long period of time. The potential flow is determined and then used to describe the pressure field evolution around the collapsing bubble. One attractive advantage of the method is its small computer run time. Less than fourty seconds of a Univac 1110 are needed to describe the whole bubble collapse as well as the pressure field.

FORMULATION OF THE PROBLEM

Let us consider the classical problem of the collapse of an initially spherical bubble near a solid wall. R_o is the initial radius of the sphere and ℓ_o is

the initial distance from its center to the solid wall. Due to a change in the ambient pressure $P_\infty(t)$, the bubble shape changes. Our aim is to determine, at a subsequent time t, the equation of the bubble wall, $R(\theta,t)$, as well as, the pressure field around it, $p(r,\theta,t)$. To do so, let $O_oX_oY_oZ$ be the initial coordinate system and OXYZ a coordinate system moving in the z direction. If b(t) is the distance OO_o, the distance from the origin to the wall at the time t is given by $\ell(t) = \ell_o - b(t)$. A point M on the bubble surface is defined by the angle θ (Fig. 1) and the distance $R(\theta,t)$ from O.

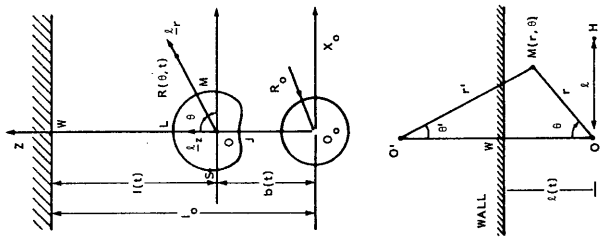

FIGURE 1 - DEFINITION OF DIFFERENT CHARACTERISTIC LENGTHS

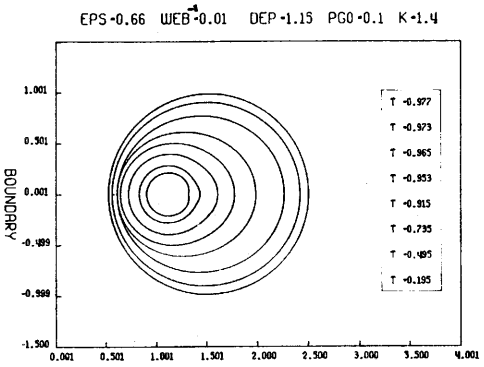

FIGURE 2 -
SHAPE OF THE BUBBLE AT DIFFERENT TIMES

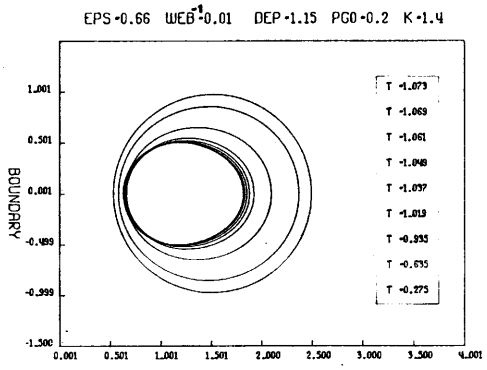

FIGURE 3 -
SHAPE OF THE BUBBLE AT DIFFERENT TIMES

If the fluid is assumed to be inviscid and the flow irrotationnel there exists a velocity potential ϕ such that the velocity field is given by $\underline{V} = \underline{\nabla}\phi$. If the fluid is in addition incompressible, it satisfies the Laplace equation,

$$\Delta\phi = 0 \quad . \tag{1}$$

To determine the bubble wall motion one has to solve (1) subjected to the following kinematic and dynamical conditions on the bubble surface and on the solid wall:

$$\underline{\nabla}\phi \cdot \underline{n}\big|_{r = R(\theta,t)} = [\dot{R} \cdot \underline{e}_r + \dot{b} \cdot \underline{e}_z] \cdot \underline{n} \tag{2}$$

$$\rho[\dot{\phi} - \dot{b}\,\underline{e}_z \cdot \underline{\nabla}\phi + \tfrac{1}{2}|\underline{\nabla}\phi|^2]_{r = R(\theta,t)} = P_\infty(t) - P_g(t) - P_v + 2\gamma C(\theta,t) \tag{3}$$

$$\underline{\nabla}\phi \cdot \underline{n}\big|_{r = \ell(t)/\cos\theta} = 0 \quad , \tag{4}$$

where C and $\underline{n}$ are respectively the curvature of the bubble surface and its unit normal vector at the point $M(\theta,t)$. γ is the surface tension and dots denote time differentiation. ϕ and the operator ∇ are expressed in the moving system OXYZ. P_∞, P_v and P_g are the imposed ambient pressure, the vapor pressure and the pressure of the gas inside the bubble. If we assume a polytropic behavior, P_g is

related to its initial value by the equation

$$P_g(t) = P_{g_o} \frac{R_o^{3k}}{V(t)^k} \tag{5}$$

where $V(t)$ is the volume of the bubble at the time t, and k is the polytropic coefficient ($1 < k < c_p/c_v$).

To these conditions, we have to add the initial condition and the boundary condition at infinity:

$$\begin{aligned} &\phi(r,\theta,o) = 0 \\ &P_\infty(o) = P_o = P_{g_o} + P_v - \frac{2\gamma}{R_o} \\ &\lim_{r \to \infty} \phi(r,\theta,t) = 0 \end{aligned} \tag{6}$$

The pressure field is then determined by the Bernoulli equation which can be written in the fixed system $O_o X_o Z$ as follows:

$$p(r,t) = -\dot{\phi}_f - \tfrac{1}{2}|\underline{\nabla}_f \phi_f|^2 + P_\infty(t) \tag{7}$$

In the moving system this expression becomes:

$$p(r,t) = -\dot{\phi} + \dot{b}\, \underline{e}_z \cdot \underline{\nabla}\phi - \tfrac{1}{2}|\underline{\nabla}\phi|^2 + P_\infty(t) \tag{7}$$

With no further simplifications or assumptions, this general problem is not easily solved analytically. As mentioned above, numerical computations, can be used, the most attractive ones being based on a variational formulation. However, when the ratio R_o/ℓ_o is small, analytical calculations using matched asymptotic expansions dramatically simplify the problem leading to a low time-consuming numerical resolution.

MATCHED ASYMPTOTIC PROBLEM

When the orders of magnitude of R_o and ℓ_o are different (i.e., $R_o/\ell_o = \varepsilon \ll 1$), the problem has two different characteristic lengths, and depending on whether one is interested in the vicinity of the bubble "inner region", or in the vicinity of the solid wall "outer region", R_o or ℓ_o should be respectively choosen as the length scale, L. By doing so, the problem (1) to (6) is divided into two easier subproblems, the "inner" ($L = R_o$) and the "outer" ($L = \ell_o$), with matching conditions in between. Before giving the details let us notice that, to the first order of approximation ($\varepsilon = 0$) in the inner problem the solid wall is effectively at infinity. The bubble reacts to a change $P_\infty(t)$ in the ambient pressure as if it were in an infinite medium. It therefore behaves spherically, its wall motion $a_o(t)$ being given by the Rayleigh-Plisset (2) equation. To the same order of approximation, in the outer problem the bubble appears as a single point and the boundary conditions on its surface are to be replaced by the matching conditions with the inner problem. That is to say, the value of the potential when $\bar{r}(=r/\ell_o)$ tends to zero, is equal to the limit of the inner potential, where $\tilde{r}(=r/R_o)$ tends to infinity. Thus the bubble appears in the outer problem, as a spherical singularity of strength $q_o(t) = a_o^2(t) \cdot \dot{a}_o(t)$ centered at 0. The outer problem is then that of a source in the presence of a solid wall. The solution is easily obtained by the use of the method of images: The total flow is that due to the superposition of two sources - one the actual source at 0 and the other an identical one symmetrical to 0 with respect to the wall. Turning back to the

inner problem we can now solve the second order of approximation. Here the at-infinity conditions are given by the matching condition with the first order of approximation of the outer solution (details below), and by the application of the principle of less degeneracy. The successive order of approximation are solved in a similar manner in the two regions, the solutions being subjected to the following matching condition

$$\lim_{\bar{r} = r/\ell_o \to o} \phi_{out} = \lim_{\tilde{r} = r/R_o \to \infty} \phi_{in} \tag{8}$$

NON-DIMENSIONALIZATIONS

In order to make asymptotic expansions (and thus to compare orders of magnitudes) an accurate choice of characteristic scale variables is fundamental. For the length scales the choice is obvious: R_o in the inner problem, ℓ_o in the outer. The time scale has to be the same for the two problems and, since we are interested in the collapse history, the Rayleigh time based on R_o and the characteristic value of the imposed pressure perturbation, Δp, is taken as this time scale:

$$T = R_o \sqrt{\rho/\Delta P} \quad . \tag{9}$$

Δp, which is also taken as the characteristic scale for the pressures, can be defined as the difference between the maximum value of $P_\infty(t)$ and the initial value $P_\infty(o) = P_o$

$$\Delta P = P_{max} - P_o \quad . \tag{10}$$

If surface tension is neglected and if the cavity contains only liquid vapor, then $P_o = P_v$ and T is the classical Rayleigh time. In the more general case considered here P_o is given by (6).

The only variable left is the characteristic velocity potential Φ_o. As we have mentioned before, in both regions the flow in the first approximation is due to the presence of a source (and its image for the outer problem) of strength $q_o(t)$ (characteristic scale R_o^3/T). Then, the velocity potential has the scale $q_o(t)/r$. That is to say, $\Phi_o = R_o^2/T$ for the inner problem and $\Phi_o = R_o^3/\ell_o T$ for the outer problem.

With these characteristic scales, non-dimensional variables all of order unity are introduced through the following definitions, where bars denote outer non-dimensional variables and tildes inner ones.

$$\begin{aligned}
&\tilde{r} = r/R_o \quad ; \quad \bar{r} = r/\ell_o \\
&\tilde{\phi} = \phi T/R_o^2 \; ; \quad \bar{\phi} = \varepsilon\, \phi\, T/R_o^2 \\
&\tilde{p}(t) = \bar{p}(t) = (p(t) - P_o)/\Delta P \\
&\tilde{t} = \bar{t} = t/R_o \sqrt{\rho/\Delta P} \\
&\bar{\ell} = \ell/\ell_o \\
&\tilde{b} = b/R_o \quad ; \quad \bar{b} = b/\ell_o
\end{aligned} \tag{11}$$

Each of the unknowns is then expanded in power series of ε as follows:

$$\bar{\phi} = \bar{\phi}_o + \varepsilon\bar{\phi}_1 + \bar{\varepsilon}^2\bar{\phi}_2 + \varepsilon^3\bar{\phi}_3 + \ldots$$
$$\tilde{\phi} = \tilde{\phi}_o + \varepsilon\tilde{\phi}_1 + \varepsilon^2\tilde{\phi}_2 + \varepsilon^3\tilde{\phi}_3 + \ldots$$

$$\tilde{b} = \tilde{b}_o + \varepsilon\tilde{b}_1 + \varepsilon^2\tilde{b}_2 + \varepsilon^3\tilde{b}_3 + \ldots$$

$$\tilde{R} = \tilde{a}_o + \varepsilon\tilde{R}_1 + \varepsilon^2\tilde{R}_2 + \varepsilon^3\tilde{R}_3 + \ldots$$

ANALYTICAL SOLUTION

First Order of Approximation (ε^o)

As stated before, the bubble behaves spherically to the first order of approximation, and its radius is given by the following non-dimensional Rayleigh-Plesset equation:

$$\tilde{a}_o \ddot{\tilde{a}}_o + \frac{3}{2}\dot{\tilde{a}}_o^2 = -\tilde{p}_\infty(\tilde{t}) + P(\tilde{a}_o^{-3k} - 1) + W_e^{-1}(\tilde{a}_o^{-3k} - \tilde{a}_o^{-1}) \tag{12}$$

where

$$W_e = R_o \cdot \Delta P/2\gamma$$

$$P = \frac{P_o - P_v}{\Delta P} = \frac{P_{g_o}}{\Delta P} - W_e^{-1} = \bar{P}_{g_o} - W_e^{-1} \tag{13}$$

The parameter P is a measure of the initial non-dimensional gas pressure inside the bubble. The potential flow in the inner problem can then be written:

$$\tilde{\phi}_o = \frac{-\tilde{a}_o^2\dot{\tilde{a}}_o}{\tilde{r}} = \frac{-\tilde{q}_o(\tilde{t})}{\tilde{r}} \quad , \tag{14}$$

In the outer problem, the potential flow is that due to the superposition of two symmetrical sources relative to the wall (Fig. 1) and can be written:

$$\bar{\phi}_o = -\tilde{q}_o(\tilde{t})\left[\frac{1}{\bar{r}} + \frac{1}{\bar{r}'}\right] \quad . \tag{15}$$

To this order, due to the spherical symmetry of the problem, no bubble motion occurs and if we fix the origin of coordinates to the bubble we can write:

$$\bar{\ell}_o = 1 \quad , \quad \tilde{b}_o = 0 \tag{16}$$

Second Order of Approximation (ε^1): Lengthening Effect

The matching condition (8) shows that the first correction to the order-zero inner solution (14) is of order ε. Definitions (11) being taken into account, Equation (8) can be written:

$$\lim_{\bar{r}\to\infty}(\tilde{\phi}_o + \varepsilon\tilde{\phi}_1 + \ldots.) = \varepsilon \lim_{\bar{r}\to\infty}(\bar{\phi}_o + \varepsilon\bar{\phi}_1 + \ldots.)$$

which with (15) implies the already-known condition,

$$\lim_{\tilde{r}\to\infty} \tilde{\phi}_o = 0 \quad ,$$

as well as

$$\lim_{\tilde{r}\to\infty} \tilde{\phi}_1 = \frac{\tilde{q}_o(\tilde{t})}{2} \quad . \tag{17}$$

$\tilde{\phi}_1$ has to satisfy the Laplace equation, as well as the boundary conditions on the bubble wall (the contribution to order ε of the expansion of (2) and (3) non-

dimensionalized).

To this order all boundary conditions are spherical so that the solution $\tilde{\phi}_1$ can be written as:

$$\tilde{\phi}_1 = -\frac{\tilde{q}_1}{\bar{r}} - \frac{\tilde{q}_o}{2} \tag{18}$$

where $\tilde{q}_o$ and $\tilde{q}_1$ are functions of time. $\tilde{q}_o$ has been defined earlier, (14), and

$$\tilde{q}_1 = \tilde{a}_o^2 \dot{\tilde{a}}_1 + 2\tilde{a}_o \dot{\tilde{a}}_o \tilde{a}_1 \quad . \tag{19}$$

The first spherical correction, $\tilde{a}_1$, of the bubble radius is obtained by solving the following differential equation.

$$\tilde{a}_o \ddot{\tilde{a}}_1 + 3\dot{\tilde{a}}_o \dot{\tilde{a}}_1 + \tilde{a}_1 \left(\ddot{\tilde{a}}_o - \frac{2W_e^{-1}}{\tilde{a}_o^2} + 3k \frac{\bar{P}_{g_o}}{\tilde{a}_o^{3k+1}} \right) = -\frac{\dot{\tilde{q}}_o}{2} \tag{20}$$

$$\tilde{R}_1(\theta, \tilde{t}) = \tilde{a}_1(\tilde{t})$$

If the surface tension and the pressure of noncondensable gas are neglected, Equations (20) and (12) can be integrated to give the corrected period of oscillation of the bubble, which can be written:

$$\bar{\tau} = \bar{\tau}_o + \varepsilon \bar{\tau}_1 = 0.915 \left(1 + \frac{\varepsilon}{4} \int_o^1 \tilde{a}_o d\tilde{t} \right) \tag{21}$$

where $\bar{\tau}_o$ is the nondimensional time needed for a spherical void to collapse. A solid wall is therefore seen to have a lengthening effect on the bubble collapse time (a free surface gives a shortening effect). This result has been predicted by energy considerations by Herring (10) as early as 1941.

The outer solution of the problem is obtained by the use of the method of images, which consists of adding a symmetrical image to the correction-source, to give:

$$\bar{\phi}_1 = -\tilde{q}_1 \left[\frac{1}{\bar{r}} + \frac{1}{\bar{r}'} \right] \tag{22}$$

As the problem is still spherical to this order, no motion is involved, and

$$\bar{\ell}_1 = \tilde{b}_1 = 0 \tag{23}$$

Third Order of Approximation (ε^2): Motion and First Non-Spherical Deformation

The first non-spherical term in the equations appears to the order ε^2, in the expansion of the matching condition (8). This term varies as $\cos\theta$. Since the non spherical terms involving the motion of the origin of coordinates in the boundary conditions on the bubble ((2) and (3)) are also of the form $\cos\theta$, the principle of less degeneracy leads to the choice,

$$\tilde{b} = \varepsilon^2 \tilde{b}_2 + \ldots .$$

The equations to this order takes then the form:

$$\Delta\tilde{\phi}_2 = 0 \tag{24}$$

$$\left.\frac{\partial\tilde{\phi}_2}{\partial\tilde{r}}\right|_{\tilde{r}=\tilde{a}_o} = 2\,\tilde{R}_2\,\frac{\dot{\tilde{a}}_o}{\tilde{a}_o} + \dot{\tilde{R}}_2 + \dot{\tilde{b}}_2\cos\theta + F_1(\tilde{a}_1,\tilde{a}_o) \tag{25}$$

$$-\tilde{a}_o\left.\frac{\partial\tilde{\phi}_2}{\partial\tilde{r}} - \frac{\partial\tilde{\phi}_2}{\partial\tilde{t}}\right|_{\tilde{r}=\tilde{a}_o} = \tilde{R}_2\ddot{\tilde{a}}_o + \frac{W_e^{-1}}{\tilde{a}_o^{\,2}}\left(2\,\tilde{R}_2 + \frac{\partial\tilde{R}_2}{\partial\theta}\cot g\theta + \frac{\partial^2\tilde{R}_2}{\partial\theta^2} - \frac{2a_1^{\,2}}{\tilde{a}_o^{\,2}}\right) - \dot{\tilde{a}}_o\dot{\tilde{b}}_2\cos\theta + F_2(\tilde{a}_1,\ \tilde{a}_o,\ \tilde{P}_{g_o},k) \tag{26}$$

$$\lim_{\tilde{r}\to\infty}\tilde{\phi}_2 = -\frac{\tilde{q}_o}{4}\,\tilde{r}\cos\theta + \frac{\tilde{q}_1}{2} \tag{27}$$

where F_1 and F_2 are known functions of $\tilde{a}_1$, $\tilde{a}_o$, k and $\tilde{P}_{g_o}$.

This problem is more complex than those already solved in the two preceding orders. A solution can be obtained by means of an infinite spherical harmonic series expansion of $\tilde{\phi}_2$. Fortunately, due to the condition (27) and to the initial condition $\tilde{\phi}_2(r,\theta,o) = 0$, all the terms of the expansion are shown to be identically zero except the following ones:

$$\tilde{\phi}_2 = -\frac{\tilde{q}_2}{\tilde{r}} + \left(\frac{\tilde{h}_2}{\tilde{r}^2} + \frac{\tilde{q}_o}{4}\,\tilde{r}\right)\cos\theta - \frac{\tilde{q}_1}{2}\ . \tag{28}$$

This leads to,

$$\tilde{R}_2(\theta,t) = \tilde{a}_2(t) + \tilde{f}_2(t)\cos\theta\ . \tag{29}$$

$\tilde{a}_2$ and $\tilde{f}_2$ are given by the following differential equations:

$$\tilde{a}_o\ddot{\tilde{a}}_2 + 3\dot{\tilde{a}}_o\dot{\tilde{a}}_2 + \tilde{a}_2\cdot\left(\ddot{\tilde{a}}_o - \frac{2W_e^{-1}}{\tilde{a}_o^{\,2}} + \tilde{P}_{g_o}\frac{3k}{\tilde{a}_o^{\,3k+1}}\right) = -\frac{\dot{\tilde{q}}_1}{2} + F_3(\tilde{a}_o,\tilde{a}_1,\ W_e^{-1},\tilde{P}_{g_o},k) \tag{30}$$

$$\tilde{a}_o\ddot{\tilde{f}}_2 + 3\dot{\tilde{a}}_o\dot{\tilde{f}}_2 = -\tilde{a}_o\ddot{\tilde{b}}_2 - 3\dot{\tilde{a}}_o\dot{\tilde{b}}_2 - \frac{3}{4}\left(\dot{\tilde{a}}_o\tilde{q}_o + \tilde{a}_o\dot{\tilde{q}}_o\right) \tag{31}$$

Once $\tilde{a}_2$ and f_2 are known, $\tilde{q}_2$ and $\tilde{h}_2$ are given by the following relations,

$$\tilde{q}_2 = 2\,\frac{\tilde{a}_1}{\tilde{a}_o}\,\tilde{q}_1 + \left(2\,\frac{\tilde{a}_2}{\tilde{a}_o} - 3\,\frac{\tilde{a}_1^{\,2}}{\tilde{a}_o^{\,2}}\right)\tilde{q}_o + \dot{\tilde{a}}_2\tilde{a}_o^{\,2} \tag{32}$$

$$\tilde{h}_2 = -\tilde{q}_o\left(\frac{\tilde{a}_o^{\,3}}{8} + \tilde{f}_2\right) - \frac{\tilde{a}_o^{\,3}}{2}\left(\dot{\tilde{f}}_2 + \dot{\tilde{b}}_2\right)\ . \tag{33}$$

The only remaining unknown, needed to solve equations (30) and (31) is the imposed motion of the origin of coordinates $\tilde{b}_2(t)$. The aim of this arbitrary motion, as stated before, is to provide at each time $\tilde{t}$ a system of coordinates which can describe the bubble wall equation correctly. With no motion of O, the part of the bubble surface farthest from the wall can reach O early in the collapse history. For subsequent times, O is outside the domain bounded by the bubble surface and the spherical coordinate system used (r,θ,ϕ) is no longer

adequate to describe this surface. Therefore, the coordinate motion should be chosen in order to delay this limit, if not to avoid it. The first idea which comes to mind is to attach O to the center of gravity G of the bubble by writing its equation of motion. This motion is such that the net pressure thrust on the massless moving bubble is zero. The equation obtained is not an additional one and gives again (3) (or to this order (30) and (31)). Thus, the position of G is known once the whole problem is solved. An iterative procedure can be used by taking the position of the center of gravity of the bubble, at a given time step, as the new origin for the following step. Another approach has been used here because it appeared more practical. If a cavity is assumed to remain spherical while oscillating near a solid wall as a source of strength $\tilde{q}_o(t)$, its center moves toward the wall with the velocity $\tilde{b}_s(\tilde{t})$ given by:

$$2\tilde{a}_o\ddot{\tilde{b}}_s + 6\dot{\tilde{a}}_o\dot{\tilde{b}}_s = -\dot{\tilde{a}}_o\tilde{q}_o - \tilde{a}_o\dot{\tilde{q}}_o \tag{34}$$

An equivalent equation has been used in the literature to determine the bubble motion. To obtain (34), only the source-image relative to the wall is taken into account. The images relative to the bubble wall are neglected and hence the conditions (3,4) on the bubble surface are not satisfied. A motion of the origin of coordinates proportional to $\tilde{b}_s$, such that $\tilde{b}_2 = D_{ep} \cdot \tilde{b}_s$, is applied and gives good results for $1 < \lambda < 1.5$.

Order ε^3 and Following

As we have seen above, the choice of $\tilde{b}$ is somewhat arbitrary. We will then restrict the motion of the origin to $\tilde{b}(\tilde{t})$ and treat the following orders of approximation with no correction of this motion. One can show that to each order, as for the preceeding orders, the radius $R_n(\theta,t)$ is of the form:

$$R_n(\theta,\tilde{t}) = \tilde{a}_n(\tilde{t}) + \tilde{f}_n(\tilde{t})\cos\theta + \tilde{g}_n(\tilde{t})\ P_2(\cos\theta) + \ldots . \tilde{y}_n(\tilde{t})P_{n-1}(\cos\theta)$$

where $P_n(\cos\theta)$ is the Legendre polynomial of order n. For n = 3, we have:

$$R_3(\theta,t) = \tilde{a}_3(\tilde{t}) + \tilde{f}_3(\tilde{t})\ \cos\theta + \tilde{g}_3(t) \cdot (3\cos^2\theta - 1)/2 \tag{35}$$

$\tilde{a}_3(\tilde{t})$, $\tilde{f}_3(\tilde{t})$ and $\tilde{g}_3(\tilde{t})$ are obtained by solving the following differential equations:

$$\begin{aligned}\tilde{a}_o\ddot{\tilde{a}}_3 + 3\dot{\tilde{a}}_o\dot{\tilde{a}}_3 + \tilde{a}_3(\ddot{\tilde{a}}_o - 2W_e^{-1}\tilde{a}_o^{-2} + 3K\tilde{P}_{g_o} \cdot \tilde{a}_o^{-3k-1}) \\ = F_4(\tilde{a}_0,\ \tilde{a}_1,\ \tilde{a}_2,\ W_e^{-1},\ \tilde{P}_{g_o})\end{aligned} \tag{36}$$

$$\tilde{a}_0\ddot{\tilde{f}}_3 + 3\dot{\tilde{a}}_0\dot{\tilde{f}}_3 = F_5(\tilde{a}_0,\ \tilde{a}_1,\ \tilde{f}_2) \tag{37}$$

$$\tilde{a}_0\ddot{\tilde{g}}_3 + 3\dot{\tilde{a}}_0\dot{\tilde{g}}_3 - \tilde{g}_3(\ddot{\tilde{a}}_0 - 12W_e^{-1}\tilde{a}_0^{-2}) = -5(\tilde{a}_0^{\,4}\ddot{\tilde{a}}_0 + 4\tilde{a}_0^{\,3}\dot{\tilde{a}}_0^{\,2})/8 \tag{38}$$

where F_4 and F_5 are known functions of variables determined in the preceding orders of approximation. For the sake of concisness the complete expressions are not given here but can be found along with more details of the calculations in (11).

Pressure Field

To sum up, the velocity potential in the outer problem can be written as follows:

$$\begin{aligned}\bar{\phi}(\bar{r},\theta,t) = &-(\tilde{q}_0 + \varepsilon\tilde{q}_1 + \varepsilon^2\tilde{q}_2 + \varepsilon^3\tilde{q}_3 + \varepsilon^4\tilde{q}_4)(\bar{r}^{-1} + \bar{r}'^{-1}) \\ &+ (\varepsilon^3\tilde{h}_2 + \varepsilon^4\tilde{h}_3)(\bar{r}^{-2}\cos\theta - \bar{r}'^{-2}\cos\theta') \\ &+ \varepsilon^4\tilde{K}_3(\bar{r}^{-3}P_2(\cos\theta) + \bar{r}'^{-3}P_2(\cos\theta')) + O(\varepsilon^4)\end{aligned} \tag{39}$$

The pressure field is obtained by replacing $\bar{\phi}$ by its value in the Bernoulli equation to give:

$$\bar{p} = A_s \left[\varepsilon \dot{\tilde{q}}_0 + \varepsilon^2 \dot{\tilde{q}}_1 + \varepsilon^3 \dot{\tilde{q}}_2 + \varepsilon^4 \dot{\tilde{q}}_3 \right] - \varepsilon^4 \left[(\dot{\tilde{q}}_0 \tilde{\chi}_2 + \tilde{q}_0 \dot{\tilde{\chi}}_2)\, E + \dot{\tilde{h}}_2 (\cos\theta \cdot r^{-2} - B) + \tilde{q}_0 \dot{\tilde{\chi}}_2 \cos\theta\, A_e - \tilde{q}_0 \dot{\tilde{\chi}}_2 \sin\theta\, A_F + \tilde{q}_0^{\,2} A_p \right] + O(\varepsilon^4) \tag{40}$$

where

$$A_s = \bar{r}^{-1} + \bar{r}'^{-1} \quad ; \quad A_e = \bar{r}^{-2} + (\bar{r} - 2\cos\theta)\, \bar{r}'^{-3}$$
$$E = 2(2-\bar{r})\cos\theta \cdot \bar{r}'^{-3} \quad ; \quad A_F = 2\sin\theta \cdot \bar{r}'^{-3} \tag{41}$$
$$B = (2 - \bar{r}\cos\theta)\, \bar{r}'^{-3} \quad ; \quad A_p = (A_e^{\,2} + A_F^{\,2})/2$$

Once the evolution of the surface of the bubble and the velocity potential are determined, (41) allows a complete description of the pressure field and of its evolution with time.

NUMERICAL RESULTS

The equations (12),(20),(30),(36) to (38) constitute a system of seven equations with seven unknowns. Each of these equations is a differential equation of the second order which can be solved numerically by a Runge-Kutta procedure. Particularily the Rayleigh Plesset equation (12), and the origin of coordinates motion equation (34) are independent and can be solved easily to give $\tilde{a}_0$ and $\tilde{b}_2$. Equations (20) and (38) which depend on $\tilde{a}_0$ and equation (31) which depend on $\tilde{a}_0$ and $\tilde{b}_2$ can then be solved by the same procedure. The results are used to solve the remaining equations. This "multi-Runge Kutta" procedure is convergent and gives in few seconds of run on a Univac 1110 computer the collapse history of the bubble in some two thousands steps of time.

The results are illustrated in Figures 2 and 3. In both figures the initial bubble-center to wall distance is 1.5 R_o. This is a classical case which was investigated in previous publications (5,6,7). The numerical results of (5) were checked experimentally in (3). As can be seen from the comparison between the two figures the influence of $\bar{P}_{g_o}$ is very important. $\bar{P}_{g_o} = 0.2$ gives a cushionned collapse followed by a rebound without the formation of a re-entering jet. On the other hand when $\bar{P}_{g_o} = 0.1$, a re-entering jet is clearly formed. At the time-step following $t = 0.977\, (\rho/P_o - P_v)^{\frac{1}{2}}$, the motion of the jet overtakes that of the origin of coordinates, and the method no longer describes the bubble equation correctly. In order to investigate the influence of different parameters on the bubble wall motion, Figures 4 and 5 compare the motion of the re-entering point on the bubble surface (point J in Figure 1) in different cases. Figures 6 and 7 compare the motion of the origin of coordinates O. We can see from Figure 4, that decreasing the initial pressure of noncondensable gases inside the bubble $\bar{P}_{g_o}$ is as effective in increasing the violence of the bubble collapse as decreasing the bubble wall distance. This result also applies to the pressure field generated around the bubble, and thus to the erosive effect of collapse. Such behavior is expected since the gas acts as a spring cushioning the bubble implosion. The importance of the law of behavior of this gas, showed analytically in (4), is remarkably illustrated in Figure 5 where the re-entering jet behavior is completely different between K = 1 and K = 1.4. However, the interpretation of the result is complicated: One would expect a faster collapse for the isothermal law. This is the case for the first order of approximation a_o. However, the corrections a_1, a_2, a_3, which are inversely dependant on a_o, are greater than in the more realistic adiabatic case. The isothermal collapse remains more energetic since the attraction of the bubble towards the wall is much higher (Fig. 7). This is reflected in the results obtained for the pressure field. Let us note, however, that the solution in the isothermal case looses its validity earlier in the collapse history

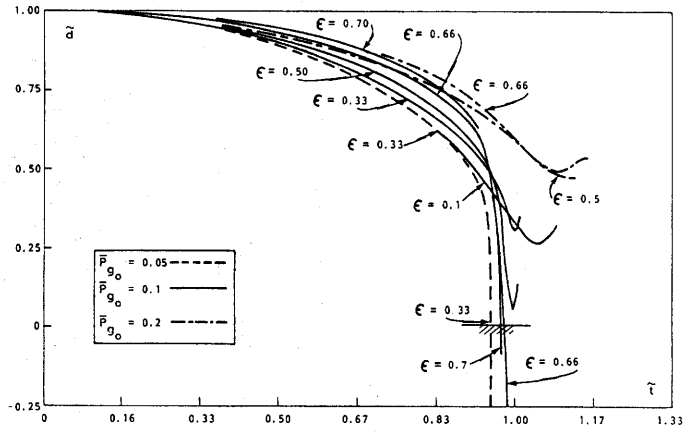

FIGURE 4 - MOTION OF THE REENTERING POINT ON THE BUBBLE SURFACE . INFLUENCE OF ϵ AND $\bar{P}_{g_o}$, D_{ep} = 1.15, W_e^{-1} = 0.01

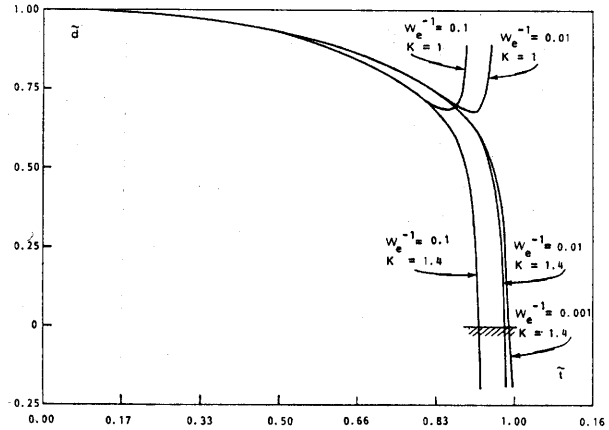

FIGURE 5 - MOTION OF THE REENTERING POINT ON THE BUBBLE SURFACE INFLUENCE ON K AND W_e^{-1}. D_{ep} = 1.15, ϵ = 0.66, $\bar{P}_{g_o}$ = 0.1

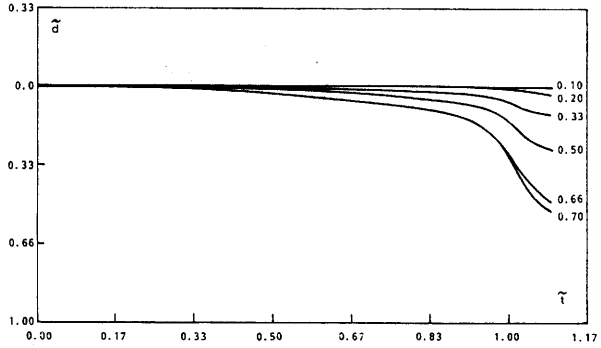

FIGURE 6 - BUBBLE CENTER MOTION - INFLUENCE OF ϵ

D_{ep} = 1.15 $\bar{P}_{g_o}$ = 0.1 W_e^{-1} = 0.01 K = 1.4

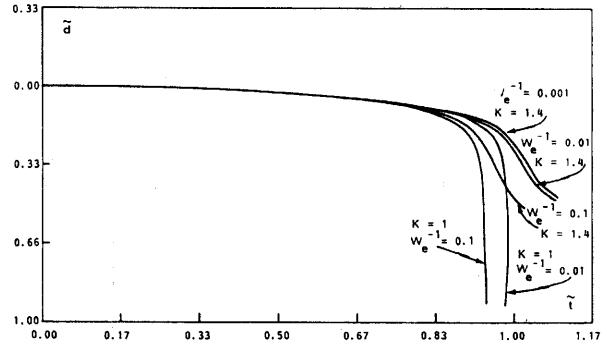

FIGURE 7 - BUBBLE CENTER MOTION - INFLUENCE OF K, W_e^{-1}

D_{ep} = 1.15 , $\bar{P}_{g_o}$ = 0.1 , ϵ = 0.66

since the ratio of the bubble radius to its distance from the wall increases rapidly.

The influence of the surface tension can be deduced from Figs. 5 and 7. For high Weber numbers (W_e>100) the motion of the re-entering point and of the center of the bubble are not very sensitive to a change of W_e. These motions become highly dependent on W_e for smaller values of this parameter. Surface tension effects are thus expected to become important with typical fluids for very small values of (R_o · ΔP). A similar effect is known for spherical bubbles. The most interesting result concerning nonspherical bubble dynamics is the influence of ε (proximity of the wall) on the behavior of the re-entering jet and on the duration of collapse. As shown above, from considerations on the spherical corrections of the Rayleigh Plesset solution, a lengthening effect on the bubble collapse time is obtained with presence of a solid wall: The increase in the bubble life is directly proportional to ε. However, one would expect intuitively that the jet velocity would increase with ε and that the time needed for this jet to reach the opposite bubble wall can be smaller than the time needed for a spherical bubble to attain its maximum radius. This reasoning has been confirmed experimentally (4,12). Figure 4 (and in more detail, Fig. 8) shows this effect: Until the latest stage of collapse, increasing ε increases, at a given time, the distance OJ (Fig. 1). This shows the tendancy towards lengthening the bubble life. However, this tendency is reversed later. The speed of the jet increases with ε and the overall effect is to shorten the time needed for the re-entering jet to pierce the bubble. At the same time the attraction of the bubble towards the wall increases (Fig. 6). The effect of ε on O_oJ is greater than that on OJ since the effects on OJ and the wall distance are then added. A similar shortening effect has been reported in the case of a moving spherical bubble (13). In Fig. 8, the evolution with time of the distances OJ, OL, OS (Fig. 1) as well as the spherical solution, a are plotted simultaneously. These lengths are respectively noted in the figure as RJ, RL, RS and AO. The lengthening effect is clearly seen on RL and would be greater if the curve represented O_oL. On the contrary the collapse is faster for OS and especially of OJ, even without taking into account the motion of the origin. Let us note, however, that this is an extreme case, corresponding to Fig. 2. For non-violent collapses (low values of ε or high values of $\bar{P}_{g_o}$) a lengthening effect exists.

In the last four figures we consider the pressure field around the collapsing bubble. This subject is a matter of concern, since earlier results seem to be contradictory. Mitchell and Hammitt (6) found that the pressure between the bubble and the wall was smaller than in an infinite medium. However Korovkin and Levkoski (13) found, without taking into account the bubble deformation that the maximum value of the pressure on the nearby wall can be much higher then in the infinite medium case, if $\bar{P}_{g_o}$ is small. Here, we confirm this result without contradicting that of (6). Fig. 9 shows the evolution with time of the pressure on the wall (point W, Fig. 1) and at two other points at a distance ℓ_o from 0 - one on the axis of symetry (noted VERT) and one in the plane parallel to the wall and passing through 0 (noted HORZ). These pressures are compared to that in an infinite medium (noted INFI). The presence of the wall greatly modifies the pressure field especially at W where the maximum pressure is two orders of magnitude higher than in the infinite medium. This maximum value drops significantly for a less violent collapse: Fig. 10 shows that for $\bar{P}_{g_o}$ = 0.2, it is only three times that in an infinite medium. For $\bar{t}$ < 1, the pressure is reduced in the presence of the wall. This explains the results of (6) where the largest time in the calculations is smaller than the limiting time after which the pressures increase. These remarks are confirmed in Figs. 11 and 12. Where the variations of the pressure perturbation $\bar{p}$ with $\bar{r}$ are represented for different angles θ, at two times (0.914 and 0.949); θ = 0 corresponds to the direction of the wall. We can see that in Fig. 11 the pressure field is smaller than that in an infinite medium and is very similar to that presented in (6). However at $\bar{t}$ = 0.949 (Fig. 12) the pressure in the entire field is higher than

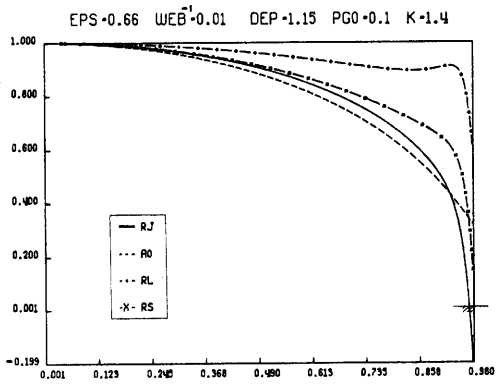

FIGURE 8 -

MOTION OF CHARACTERISTIC POINTS ON THE BUBBLE

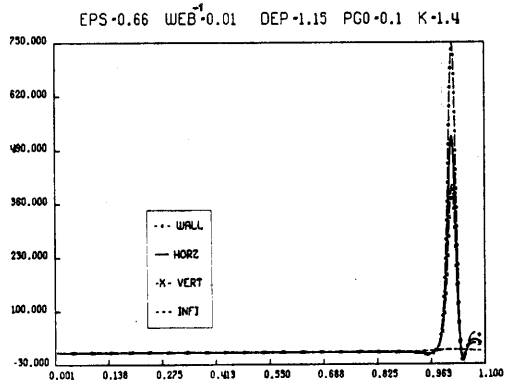

FIGURE 9 -

PRESSURE VERSUS TIME AT DIFFERENT LOCATIONS

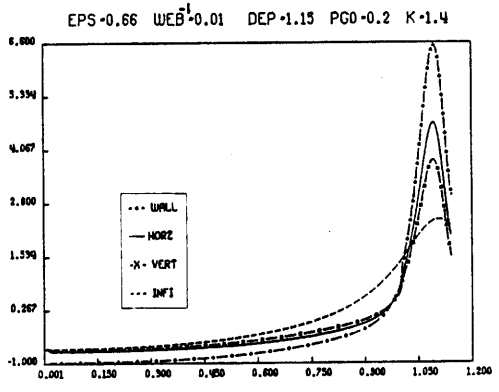

FIGURE 10 -

PRESSURE VERSUS TIME AT DIFFERENT LOCATIONS

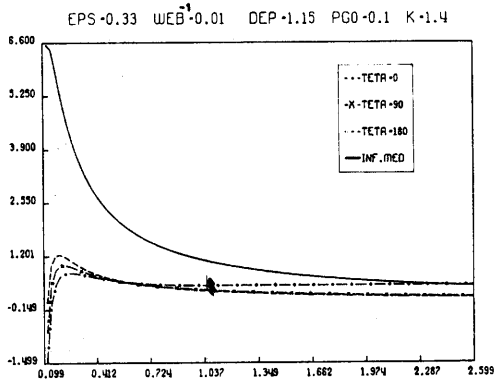

FIGURE 11 -

PRESSURE VERSUS RADIUS FOR DIF.ANGLES AT T=0.914

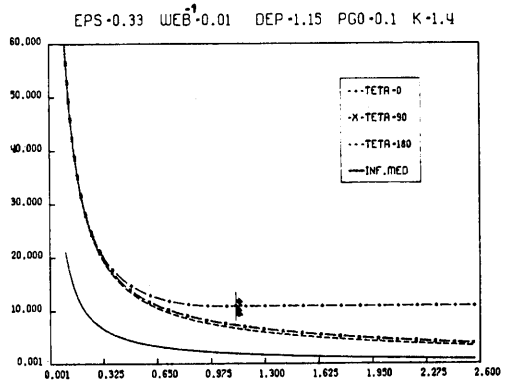

FIGURE 12 -

PRESSURE VERSUS RADIUS FOR DIF.ANGLES AT T=0.949

in the infinite medium case.

CONCLUSION

1. The method of matched asympotic expansions is seen to be successful in describing the nonspherical bubble dynamics near a solid wall, including the generated pressure field during the bubble collapse. To study more complex boundaries one need only change the second member of the differential equations solved numerically.
2. The influence of the initial gas pressure and of its law of compression is as important as the proximity of the wall (ε).
3. Higher jet velocities are obtained for greater ε and smaller $\bar{P}_{g_o}$. An overall shortening effect of the bubble collapse time is obtained for intense collapses. However this result should be moderated by the fact that for high ε the method loses its validity earlier in the collapse history.
4. Pressures, orders of magnitude higher then in the spherical case, are generated on the nearby wall when the bubble is very close to it.
5. An amelioration of the method can be obtained by a closer look at the last stage of collapse. In particular, a change in the lengths and the time scales is needed, since the problem becomes singular in time at the end of the collapse.

ACKNOWLEDGEMENTS

The main part of this work was done while both authors were members of Groupe GPI at the Ecole Nationale Supérieure de Techniques Avancées, 32 Bd Victor Paris. We wish to thank the three organizations for their support.

REFERENCES

1. Plesset, M.S. "Dynamics of Cavitation Bubbles," Journal of Applied Mechanics, Trans. ASME, No. 16, 1948, pp. 228-231.
2. Naude, C.F. and Ellis, A.T., "On the Mechanism of Cavitation Damage by Non-hemispherical Cavities Collapsing in Contact With a Solid Boundary," Journal of Basic Engineering, Trans. ASME 83, 1961, pp. 648-656.
3. Lauterborn, W. and Bolle, H., "Experimental Investigation of Cavitation Bubble Collapse in the Neighbourhood of a Solid Boundary," Journal of Fluid Mechanics, Vol 2,N.72,1975, pp. 391-399.
4. Chahine, G.L., "Etude Locale du Phénomène de Cavitation: Analyse des Facteurs Régissant la Dynamique des Interfaces," Docteur es-sciences Thesis, University Pierre et Marie Curie, Paris, March 1979.
5. Plesset, M.S. and Chapman, R.B., " Collapse of an Initially Spherical Vapor Cavity in the Neighbourhood of a Solid Boundary," Journal of Fluid Mechanics, Vol. 2, N.47, 1971, pp. 283-291.
6. Mitchell, J.M. , and Hammitt F.G., "Asymetric Cavitation Bubble Collapse," Journal of Fluids Engineering, Trans. ASME March 1973, pp. 29-37.
7. Lenoir, M., "Calcul Numérique de l'Implosion d'une Bulle de Cavitation au Voisinage d'une Paroi on d'une Surface Libre," Journal de Mêcanique, Vol. 15, N.5, 1976, pp. 725-751.
8. Shima, A. and Nakajima, K., "The Collapse of a Non-hemispherical Bubble attached to a Solid Wall," Journal of Fluid Mechanics, Vol. 2, N.80, pp.386-391.
9. Chahine, G.L. and Bovis, A.G., "Oscillation and Collapse of a Cavitation Bubble in the Vicinity of a Two-Liquid Interface," Proceedings Cavitation and Inhomogeneitis in Underwater Acoustics, Göttingen, 1980 cd. Springer-Verlag.
10. Herring, C., "Theory of the Pulsations of the Gas Bubbles Produced by an Underwater Explosion," Columbia Univ., NDRC Report C4SR20-010, 1941.
11. Bovis, A.G., "Etude Asymptotique du Phénomène de Cavitation.Cavités non spheriques," Docteur-Ingenieur Thesis, University Pierre et Marie Curie, Paris, June, 1980.
12. Chahine, G.L., and Fruman, D.H., "Dilute Polymer Solution Effects on Bubble Growth and Collapse," Journal of Physics of Fluids, Vol. 22, No. 7, pp. 1406-1407, 1979.
13. Korovkin, A.N. and Levkovskii Yu. L., "Study of the Collapse of a Cavitation Cavity Close to a Solid Wall," Journal of Engineering Sciences, Vol. 12, No. 2, pp. 246-253, 1967.